

Measurement of the Kerr Spin Parameter by Observation of a Compact Object's Shadow

Kenta HIOKI^{1,2,*} and Kei-ichi MAEDA^{1,2,†}

¹*Department of Physics, Waseda University, Okubo 3-4-1, Shinjuku, Tokyo 169-8555, Japan*

²*Waseda Research Institute for Science and Engineering, Okubo 3-4-1, Shinjuku, Tokyo 169-8555, Japan*

A black hole casts a shadow as an optical appearance because of its strong gravitational field. We study how to determine the spin parameter and the inclination angle by observing the apparent shape of the shadow, which is distorted mainly by those two parameters. Defining some observables characterizing the apparent shape (its radius and distortion parameter), we find that the spin parameter and inclination angle of a Kerr black hole can be determined by the observation. This technique is also extended to the case of a Kerr naked singularity.

PACS numbers: 04.70.-s, 95.30.Sf, 98.35.Jk

I. INTRODUCTION

It is widely believed that there exist black holes in the centers of many galaxies. Sgr A*, which is the compact radio source at the center of the Milky Way, is highly likely to be a supermassive black hole. In fact, the Newtonian orbital motion of the surrounding stars indicates the mass of the dark compact object at the Galactic center to be $M \sim 3.6 \times 10^6 M_\odot$ [1]. Since the galaxies are rotating, it is very likely that a black hole at the center of the galaxy also possesses a spin. The analysis of the iron K_α emission line in the X-ray region indicates that the fine structure of the line spectra shows the signature of the black hole spin [2, 3]. However, this is difficult to conclude because there is still some ambiguity and the result may depend on the model of a gas inflow into a black hole.

New methodological development for measuring the spin of a black hole is the grand challenge in the next generation of astronomy. The direct observation of black holes by future interferometers will become possible in the near future [4, 5, 6, 7]. In such an observation, a black hole may cast a shadow in the sky as an optical appearance due to its strong gravity, which we may call the shadow of the black hole. One has to exercise due care in the handling of the direct imaging of the shadow, where a strong gravitational lensing effect plays a crucial role. Though the theory of gravitational lensing has been well developed in the weak field approximation and has succeeded to explain many astronomical observations, we have to develop new techniques to analyze strong gravitational lensing effects, because the influence of the strong gravity appears when the photon passes the vicinity of a black hole [8, 9, 10, 11, 12]. In order to obtain definite evidence for a black hole, the direct imaging of the shadows can be efficient [13, 14, 15, 16].

To discuss such a shadow of a black hole, we have to

analyze the propagation of a light ray in the strong gravity formed by a black hole. The Kerr solution is believed to be a unique realistic and known space-time which well describes an astrophysical black hole formed by a gravitational collapse of a rotating body. It is parametrized by a spin parameter a and a gravitational mass M . The regular horizon exists if $|a| \leq M$, and we have a Kerr black hole. If this condition is not satisfied, the space-time has a naked singularity. From a theoretical standpoint, the solutions of the Einstein equations with strong gravity generally contain a space-time singularity, as a final state of a realistic gravitational collapse. If the event horizon appears and the space-time singularity is hidden, a black hole is formed. It is the so-called cosmic censorship hypothesis [17]. It implies that a naked singularity does not exist in nature. However, this hypothesis has so far not yet been proven, so a naked singularity is still one of the most important subjects of general relativity [18, 19, 20, 21]. There is still a possibility that the black hole candidates could be naked singularities.

The Kerr space-time will cast a variety of shadows which fully depend on the spin parameter, the inclination angle of a black hole, and the configuration of the light emission region. In the case that the light source is an accretion disk around a black hole, the shadow has been intensively studied numerically for various values of the black hole parameters and positions of the emission region on the disk [22, 23, 24, 25, 26, 27, 28, 29]. In general, the shape of the shadow depends on the parameters in a very complex way. To extract some information about a black hole, such as a spin parameter, from such a complicated shape, we have to find a method by which we can determine the parameters from the observed apparent shapes.

In this paper, we present how to determine a spin parameter and an inclination angle by the direct imaging of the shadows, assuming that the black hole candidate is described by the Kerr space-time. The shadows of Kerr-Newman space-times were analyzed in [30, 31, 32]. It was shown that there are sensible differences between the shape of the shadow of a Kerr-Newman black hole and that of a naked singularity. Here, by reanalyzing

*Electronic address: hioki@gravity.phys.waseda.ac.jp

†Electronic address: maeda@waseda.jp

the shadows more elaborately, we propose a method to determine those parameters and discuss how one can distinguish black holes from naked singularities for a wide range of parameters. It may allow us to rule out the possibility by observation that the black hole candidate is a naked singularity.

This paper is organized as follows. In Sec. II, we briefly summarize null-geodesics in a Kerr space-time, and define the apparent shape of a collapsed object. In Sec. III, we introduce two observables and discuss how to determine the spin parameter by observing those observables. The summary and remarks follow in Sec. IV. We use the geometric units, i.e., $c = G = 1$ and adopt the definition of curvatures in [33].

II. PHOTON ORBIT IN KERR SPACE-TIME AND SHADOW

A. Equations of geodesic motion

The space-time of a rotating black hole is well described by the Kerr metric in Boyer-Lindquist coordinates [34], which is given by

$$ds^2 = - \left(1 - \frac{2Mr}{\rho^2} \right) dt^2 + \frac{\rho^2}{\Delta} dr^2 + \rho^2 d\theta^2 - \frac{4Mra \sin^2 \theta}{\rho^2} dt d\phi + \frac{A \sin^2 \theta}{\rho^2} d\phi^2, \quad (1)$$

where

$$\begin{aligned} \Delta &:= r^2 - 2Mr + a^2, \quad \rho^2 := r^2 + a^2 \cos^2 \theta, \\ A &:= (r^2 + a^2)^2 - \Delta a^2 \sin^2 \theta. \end{aligned} \quad (2)$$

The parameters M and a represent, respectively, the mass and specific angular momentum of the black hole. The frame dragging effect is described by the off-diagonal components of the metric, $g_{t\phi}$. The event horizon of the black hole exists if the condition $|a| \leq M$ is satisfied. If it is not satisfied, such a space-time has a naked singularity. In this paper we discuss not only a black hole with $|a| \leq M$ but also a naked singularity with $|a| > M$.

In the Kerr space-time, there are two Killing vector fields due to the assumption of stationarity and axisymmetry of the space-time. It guarantees the existence of two conserved quantities for a geodesic motion in the Kerr space-time (the energy E and the axial component of the angular momentum L_z). We also have the Killing-Yano tensor field [17, 35],

$$\begin{aligned} f &= r \sin \theta d\theta \wedge [(r^2 + a^2) d\phi - a dt] \\ &\quad + a \cos \theta dr \wedge (dt - a \sin^2 \theta d\phi), \end{aligned} \quad (3)$$

which provides an additional conserved quantity (the so-called Carter constant \mathcal{Q}). It makes the geodesic equation of Kerr space-time integrable [36]. So, introducing two

conserved parameters ξ and η by

$$\xi = \frac{L_z}{E} \quad \text{and} \quad \eta = \frac{\mathcal{Q}}{E^2}, \quad (4)$$

we find the following null-geodesic equations:

$$\rho^2 \frac{dr}{d\lambda} = \pm \sqrt{\mathcal{R}}, \quad (5)$$

$$\rho^2 \frac{d\theta}{d\lambda} = \pm \sqrt{\Theta}, \quad (6)$$

$$\rho^2 \frac{dt}{d\lambda} = \frac{1}{\Delta} (A - 2Mra\xi), \quad (7)$$

$$\rho^2 \frac{d\phi}{d\lambda} = \frac{1}{\Delta} [2Mar + \xi \csc^2 \theta (\rho^2 - 2Mr)], \quad (8)$$

where λ is the affine parameter, and

$$\mathcal{R} := (r^2 + a^2 - a\xi)^2 - \Delta \mathcal{J}, \quad (9)$$

$$\Theta := \mathcal{J} - (a \sin \theta - \xi \csc \theta)^2, \quad (10)$$

with

$$\mathcal{J}(\xi, \eta) := \eta + (a - \xi)^2. \quad (11)$$

These two conserved parameters (ξ and η) completely determine the null-geodesic [37]. The equations for the coordinate t and ϕ are not so important when we discuss the black hole shadow below because of the space-time symmetries. \mathcal{R} and Θ must be non-negative from Eqs. (5) and (6). This condition for Θ implies the condition such that the pair of (ξ, η) satisfies the constraint $\mathcal{J} \geq 0$.

B. Apparent Shape of Collapsed Objects

Now we investigate the shadow of a collapsed object (a Kerr black hole or a Kerr naked singularity). In order to find out what such an object looks like, we first have to define the apparent shape of a shadow. In this paper, we assume that the light sources exist at infinity and are distributed uniformly in all directions. Hence the shadow is obtained by solving the scattering problem of photons injected from any points at infinity with any and every impact parameters.

We also assume that an observer stays at infinity ($r = +\infty$) with the inclination angle i , which is defined by the angle between the rotation axis of the collapsed object and the observer's line of sight. The celestial coordinates (α, β) of the observer are the apparent angular distances of the image on the celestial sphere measured from the direction of the line of sight. α and β are measured in the directions perpendicular and parallel to the projected rotation axis onto the celestial sphere, respectively.

These celestial coordinates are related to the two conserved parameters, ξ and η (and the inclination angle i), as

$$\alpha(\xi, \eta; i) := \lim_{r \rightarrow \infty} \frac{-rp^{(\varphi)}}{p^{(t)}} = -\xi \csc i, \quad (12)$$

$$\beta(\xi, \eta; i) := \lim_{r \rightarrow \infty} \frac{rp^{(\theta)}}{p^{(t)}} = (\eta + a^2 \cos^2 i - \xi^2 \cot^2 i)^{1/2},$$

where $(p^{(t)}, p^{(r)}, p^{(\theta)}, p^{(\phi)})$ are the tetrad components of the photon momentum with respect to locally nonrotating reference frames [38].

Then the shadow of the collapsed object is defined as follows: Suppose some light rays are emitted at infinity ($r = +\infty$) and propagate near the collapsed object. If they can reach the observer at infinity after scattering, then its direction is not dark. On the other hand, when they fall into the event horizon of a black hole, the observer will never see such light rays. Such a direction becomes dark. It makes a shadow. We define the apparent shape of a black hole by the boundary of the shadow [30]. The crucial orbits are the unstable spherical photon orbit (r -constant orbit), which we will define later.

In the case of a naked singularity, since there is no horizon, almost every light ray will come back to the infinity after scattering. However, in the Kerr space-time, there are two asymptotically flat regions; $r \rightarrow +\infty$ and $r \rightarrow -\infty$. Hence once the light rays cross to the region of $r < 0$ and go away to the other infinity ($r = -\infty$), they will never come back to our world ($r > 0$). As a result, we find a small dark spot, in the direction where photons escape to $r = -\infty$. One may also find a very narrow curve, which corresponds to the outer unstable spherical orbit (discussed later). There is another dark region in the case of a naked singularity. Some light rays which accidentally hit a singularity will never reach the observer. Hence on the celestial sphere, we will see a dark point, in the direction where photons hit the singularity.

In order to find the apparent shape, we first have to analyze photon orbits in a Kerr space-time. There are two important classes of photon orbits for a shadow, which we will discuss next.

C. Important Classes of Photon Orbits

Here we discuss two important classes of photon orbits: a spherical photon orbit and a principal null.

1. Spherical photon orbits

One important class is the unstable spherical orbit, which we find as follows.

If the orbit is on the equatorial plane, there is a circular orbit. The orbit is given by the equations;

$$\begin{aligned} \theta &= \frac{\pi}{2} \quad , \\ \mathcal{R}(r) &= 0 \quad , \quad \frac{d\mathcal{R}}{dr}(r) = 0. \end{aligned} \quad (13)$$

For a black hole, Eq. (13) gives the radius of the orbit as

$$r = r_{\text{circ}}^{(\pm)} := 2M \left\{ 1 + \cos \left[\frac{2}{3} \cos^{-1} \left(\mp \frac{a}{M} \right) \right] \right\}, \quad (14)$$

$$\xi = \xi_{\text{circ}}^{(\pm)} := \frac{\left[\left(r_{\text{circ}}^{(\pm)} \right)^2 + a^2 \right]}{a} - \frac{2r_{\text{circ}}^{(\pm)} \Delta(r_{\text{circ}}^{(\pm)})}{a \left(r_{\text{circ}}^{(\pm)} - M \right)}, \quad (15)$$

where the upper sign applies to direct orbits and the lower sign to retrograde orbits. In this case, the other conserved parameter η vanishes because the Carter constant \mathcal{Q} is zero.

If it is a naked singularity, we have only one circular orbit, which is a retrograde orbit with the radius

$$r = \tilde{r}_{\text{circ}}^{(-)} := 2M \left\{ 1 + \cosh \left[\frac{2}{3} \cosh^{-1} \left(\frac{a}{M} \right) \right] \right\}. \quad (16)$$

With this parameter ξ_{circ} , the photon can go around an infinite number of times on the circle with radius r_{circ} . If $|\xi|$ is slightly larger than $|\xi_{\text{circ}}^{(\pm)}|$, the photon from infinity comes close to this circular orbit, but goes back to infinity. On the other hand, if $|\xi|$ is slightly smaller than $|\xi_{\text{circ}}^{(\pm)}|$, then the photon from infinity gets into the horizon (or hits a ring singularity). It will never come back to our infinity ($r = +\infty$). Hence ξ_{circ} gives a part of the boundary of the shadow on the equatorial plane.

For more generic photon orbits, the Carter constant \mathcal{Q} does not vanish. Such orbits are not on a two-dimensional plane, but turn out to be three-dimensional. Even in that case, we can define a critical orbit which provides us the boundary of a shadow. This critical orbit is the (unstable) spherical orbit. Such an orbit is given by

$$\mathcal{R}(r) = 0 \quad , \quad \frac{d\mathcal{R}}{dr}(r) = 0, \quad (17)$$

with the additional condition that there exists some interval $I \subset [0, \pi)$ in which we find

$$\Theta(\theta) \geq 0 \quad \text{as} \quad \theta \in I. \quad (18)$$

The solution of Eq. (17), $r = r_{\text{sph}}$, gives the r -constant orbit. Although the orbit is three-dimensional and could be very complicated, it stays at the same radius. We call it a spherical orbit. The solutions of the spherical orbits form a one-parameter family. Hence adopting r_{sph} as the ‘‘parameter,’’ we find two conserved parameters of the spherical orbits from Eq. (17) as [30] [39]

$$\xi_{\text{sph}} = \frac{\left[\left(r_{\text{sph}} \right)^2 + a^2 \right]}{a} - \frac{2r_{\text{sph}} \Delta(r_{\text{sph}})}{a \left(r_{\text{sph}} - M \right)}, \quad (19)$$

$$\eta_{\text{sph}} = - \frac{r_{\text{sph}}^3 \left[r_{\text{sph}} \left(r_{\text{sph}} - 3M \right)^2 - 4a^2 M \right]}{a^2 \left(r_{\text{sph}} - M \right)^2}. \quad (20)$$

The parameter r_{sph} is constrained by the existence condition (18) with Eqs. (19) and (20).

Inserting Eqs. (19) and (20) into Eq. (11), we find

$$\mathcal{J} = \frac{4r_{\text{sph}}^2 \Delta(r_{\text{sph}})}{\left(r_{\text{sph}} - M \right)^2}. \quad (21)$$

Hence for real spherical orbits, we have to require the condition $\Delta(r_{\text{sph}}) > 0$, i.e., $r_{\text{sph}} > r_+$ or $r_{\text{sph}} < r_-$ for a black hole, where $r_{\pm} := M \pm \sqrt{M^2 - a^2}$ are the horizon radii, and any radius r_{sph} for a naked singularity. Since it is not a sufficient condition for the existence of a spherical orbit, when we draw the shadow of collapsed object in §. III, we have numerically checked whether the solution of Eq. (17) satisfies the condition (18).

Now we analyze the stability of the spherical photon orbit. The stability is important because an unstable spherical orbit can be critical just as the circular orbit, and it will provide us the boundary of the shadow.

The condition for the spherical photon orbit to be unstable is

$$\frac{d^2\mathcal{R}}{dr^2}(r_{\text{sph}}) > 0. \quad (22)$$

Assuming there exists a spherical orbit at the radius r_{sph} , we find that the condition for the orbit to be unstable is

$$r_{\text{sph}} > r_+ \quad \text{or} \quad r_{\text{sph}} < 0, \quad (23)$$

$$\text{for } M \geq |a| \text{ (a black hole) ,}$$

$$r_{\text{sph}} > r_0 \quad \text{or} \quad r_{\text{sph}} < 0, \quad (24)$$

$$\text{for } M < |a| \text{ (a naked singularity) ,}$$

where

$$r_0 := M + [M(a^2 - M^2)]^{1/3}. \quad (25)$$

For a black hole space-time, once the light rays enter into the event horizon, they never come out. Then the unstable spherical orbits inside the horizon ($r_{\text{sph}} < 0$) do not play any role for a shadow. On the other hand, in the case of a naked singularity, the inner unstable spherical orbit ($r_{\text{sph}} < 0$) is also important because some photons near this orbit may come back to the observer, while the others may not. It also gives a critical orbit.

Note that even if there is a stable spherical orbit, there is no corresponding point on the celestial sphere because any orbits near this spherical orbit never go away to infinity or come from infinity.

2. Principal null-directions

Next we consider the orbits with $\mathcal{J} = 0$. Equation (10) implies that $\theta = \theta_0$ (constant). This condition determines two conserved parameters as

$$\xi = \xi_{\text{prin}} := a \sin^2 \theta_0, \quad (26)$$

$$\eta = \eta_{\text{prin}} := -a^2 \cos^4 \theta_0. \quad (27)$$

Two tangent vectors of null-geodesics with these conserved quantities ξ_{prin} and η_{prin} are given by

$$l_{\pm}^{\mu} \partial_{\mu} = \frac{r^2 + a^2}{\Delta} \partial_t \pm \partial_r + \frac{a}{\Delta} \partial_{\phi}, \quad (28)$$

which represent the degenerate principal null-directions. It is because they satisfy

$$C_{abc[d} l_{\pm e]} l_{\pm}^b l_{\pm}^c = 0, \quad (29)$$

where C_{abcd} is the Weyl tensor. The existence of such shear-free principal null-geodesics is guaranteed in the Petrov type D space-time.

These principal null-geodesics may give just a dark point on the celestial sphere. Since $\mathcal{R} = \rho^4(\theta_0) > 0$, the geodesics has no turning point. The light rays go “straight” with a constant angle θ_0 from $r = +\infty$ to $r = -\infty$ (or hit on a singularity on the equatorial plane). Hence the light ray from the direction of $\theta_0 = \pi - i$ will never reach the observer. It constitutes a dark point. It turns out that it is involved in the dark shadow. Only the observer on the equatorial plane ($i = \pi/2$) will see a dark point (see §. III A).

III. MEASUREMENT OF SPIN PARAMETER

A. Expected apparent shapes

Analyzing the null-geodesics, we investigate the shadow of a Kerr black hole or a naked singularity. The shadow of a Kerr-Newman space-time was studied in [31, 32]. Here, we reanalyze the shadow more elaborately and see whether some information about the shape and/or the size can determine space-time parameters such as a spin.

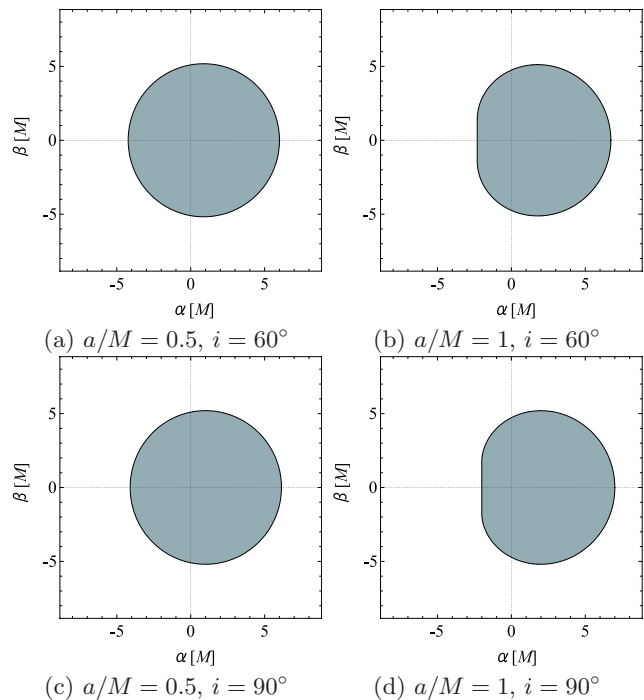


FIG. 1: The shadows of Kerr black holes. The celestial coordinates (α, β) are measured in the unit of the black hole mass M .

First we show the shadows of a Kerr black hole using Eqs. (12), (19), and (20). The light rays emitted at infinity will be captured by the black hole or be scattered back to infinity. As we mentioned, the unstable spherical orbit with a positive radius r_{sph} gives the boundary of the shadow of a Kerr black hole. Hence, it determines the apparent shape, which is shown in Fig. 1. This shaded distorted “disk” gives what we will see as a shadow of a Kerr black hole. The inside of this distorted disk is the region where null-geodesics is captured by the event horizon. If the rotation parameter a is small (e.g., $a = 0.5M$ as in Figs. 1(a) and (c)), the shape is almost a circle, while if it rotates very fast (e.g., $a = M$ as in Figs. 1(b) and (d)), the shape is distorted. The typical feature is that the left-hand side of the disk is chipped away. A dark point by the principal null-geodesic appears inside the disk in this case.

The distortion of the shape of the shadow can be understood as follows: When a black hole has a spin, the radius of the direct circular orbit decreases and then the left endpoint of the shadow moves to the right, while the retrograde’s one increases and then the right endpoint moves to the right as well (Fig. 1(c)). However, as the black hole rotates more rapidly, the radius of the direct circular orbit decreases faster than the retrograde’s one. As the result, the left endpoint of the disk moves more to the right compared with the right endpoint and then the disk is distorted especially on the left-hand side (Fig. 1(d)).

Next we show the shadows of a Kerr naked singularity in Fig. 2. In the case of a naked singularity, the event horizon does not exist and then the apparent shapes drastically change from those of a black hole (see Fig. 2). The unstable spherical photon orbit with a positive radius ($r_{\text{sph}} > r_0$) constructs an “arc” (the black solid curves in Figs. 2(a)-(d)). This is because the photons near both sides of the arc may come back to the observer due to the nonexistence of horizon. While the unstable spherical photon orbits with a negative radius ($r_{\text{sph}} < 0$) constructs a dark spot (the small distorted disk in Figs. 2(a) and (b)). The observer will never see the light rays from such directions because they escape into the other infinity ($r = -\infty$) by passing through the inside of a singular ring. It forms this dark spot. The dark point by the principal null-geodesic appears inside the spot.

When the observer is on the equatorial plane, we find that the same arc exists but the dark spot disappears. This is because the light rays in the direction of negative $r < 0$ will always hit on a ring singularity. Those null-geodesics construct a “line” (the black straight line in Figs. 2(c) and (d)). Its left endpoint corresponds to the principal null-geodesics.

Changing the inclination angle from 0° to 90° , the dark spot shrinks to a single point, which corresponds to the left endpoint of the straight line in Figs. 2(c) and (d), i.e., the principal null-geodesics.

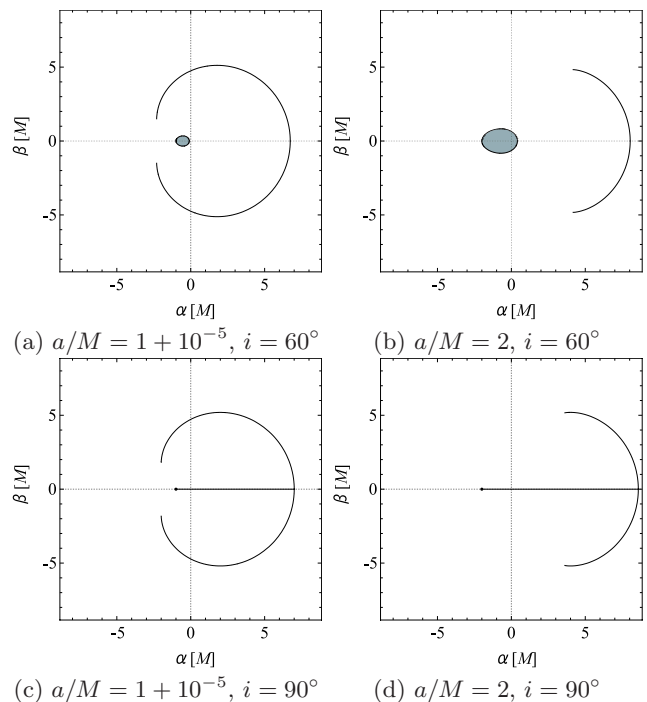


FIG. 2: The shadows of Kerr naked singularities. The arc (the black solid curves in (a)-(d)) is constructed by unstable spherical photon orbits in positive radius r_{sph} . The small distorted disk (the shaded region in (a), (b)) is constructed by the null-geodesics which escape into the other infinity ($r = -\infty$). The straight line in (c), (d) is constructed by null-geodesics which plunge into a ring singularity. The left endpoints of those lines correspond to the principal null-geodesics.

B. Observables

Thus far, we have seen that the parameters such as a spin parameter and an inclination angle determine the apparent shape of the shadow of the Kerr space-time. Now we study, inversely, whether it is possible to evaluate the spin parameter and the inclination angle by observing the shadow.

1. A black hole

In the case of a Kerr black hole, we may introduce two observables which approximately characterize the apparent shape. First we approximate the apparent shape by a circle passing through three points which are located at the top position (A), the bottom position (B), and the most right end (C) of the shadow as shown by three red points in Fig. 3. The point C corresponds to the unstable retrograde circular orbit when seen from an observer on the equatorial plane. We define the radius R_s of the shadow by the radius of this approximated circle. We also take into account the dent in the left-hand side of the shadow (see Figs. 1(b) and (d)). The size of this dent is evaluated by D_{cs} , which is the difference between the left endpoints of the circle and of the shadow (see Fig. 3).

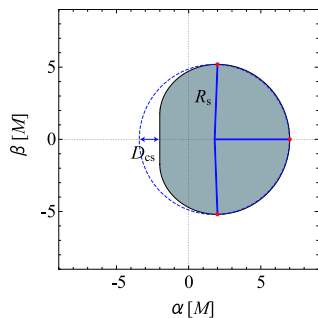
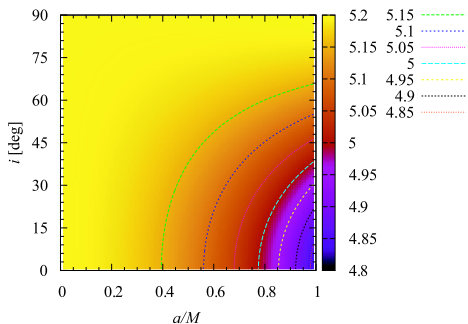
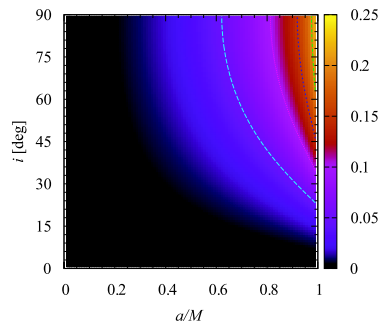


FIG. 3: The observables for the apparent shape of a Kerr black hole are the radius R_s and the distortion parameter $\delta_s := D_{cs}/R_s$, approximating it by a distorted circle, where D_{cs} is the difference between the left endpoints of the circle and of the shadow.



(a) The radius of the shadow R_s



(b) The distortion parameter of the shadow δ_s

FIG. 4: (a) The contour map of radii of the shadows of a Kerr black hole. (b) The contour map of their distortion parameters.

Then we define the distortion parameter δ_s of the shadow by $\delta_s := D_{cs}/R_s$. Thus we adopt these two variables (R_s and δ_s) as observables in astronomical observation.

We show the contour maps of the radius R_s and of the distortion parameter δ_s in terms of a spin parameter a and an inclination angle i in Fig. 4. One can see from Fig. 4(a) that the radius decreases as the spin parameter becomes larger but the inclination angle gets smaller. This is because of the following reason: The horizon radius decreases as a increases, and then the radius of the shadow also decreases when we observe near the rotation axis ($i \approx 0^\circ$). When we observe near the equatorial plane ($i \approx 90^\circ$), however, the radius of the shadow is insensitive to the rotation parameter a because $r_{\text{circ}}^{(-)}$ gets large

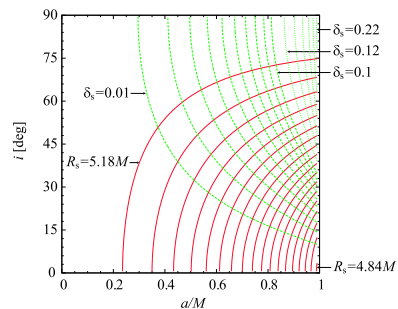


FIG. 5: The contour maps of the radius of the arc R_s (the red solid curves) and the distorted parameter δ_s (the green dashed curves). The contours are those for $R_s/M = 4.84, \dots, 5.18$, with the contour interval being 0.02, and $\delta_s = 0.01, \dots, 0.1$ and $0.12, \dots, 0.22$, with the contour intervals being 0.01 and 0.02, respectively. We can evaluate the spin parameter a of the Kerr black hole and the inclination angle i of the observer.

due to the frame dragging effect.

If one observes R_s as well as the black hole mass M and the inclination angle i , one can determine the spin parameter from this figure. On the other hand, from Fig. 4(b), we find the different tendency for the distortion of the apparent shape, i.e., δ_s increases as the spin parameter gets larger as well as the inclination angle increases. This is because we find the large distortion for the observer near the equatorial plane ($i \approx 90^\circ$) due to the frame dragging effect, but no distortion appears for the observer on the rotation axis ($i \approx 0^\circ$).

If one observes δ_s as well as M and i , one can also determine the spin parameter. However, it may be very difficult to determine the inclination angle i . Therefore we shall combine two contour maps for those observables (R_s and δ_s). The one-to-one correspondence between (a and i) and (R_s and δ_s) is very clear as shown in Fig. 5. Hence if one measures the radius R_s and the distortion parameter δ_s by observation, the spin parameter a and the inclination angle i could be determined by use of Fig. 5. For example, assuming that we know a black hole mass M , if we find two observables as $R_s = 5.1M$ and $\delta_s = 0.05$, we can conclude that $a = 0.784M$ and $i = 44.1^\circ$. So we may use this method to search for the parameters, a and i .

2. A naked singularity

In the case of a Kerr naked singularity, the shadow consists of two parts (the arc and the dark spot [or the straight line]). One interesting shape is the arc, which may not be observable because it is one-dimensional and then its measure is zero. In realistic observation, however, the neighborhood of the arc will also be darkened to be observed as a dark “lunate” shadow. If it is the case, we have a chance to observe a shadow of a naked singularity. We approximate this dark lunate shadow by the arc with the radius R_a and the central angle ϑ_a as

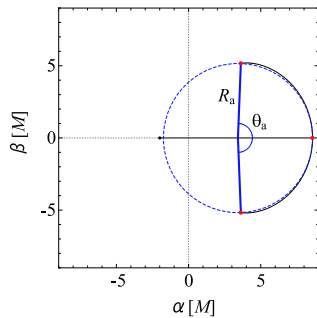


FIG. 6: The observables for the apparent shape of a Kerr naked singularity are the radius R_a and the central angle ϑ_a , approximating it by an arc.

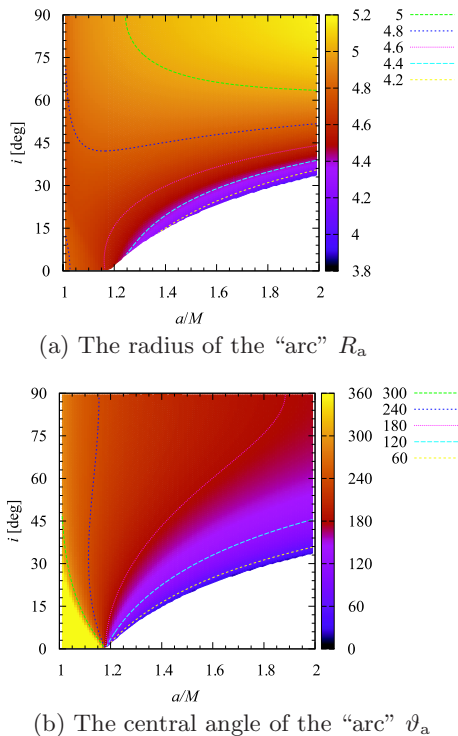


FIG. 7: (a) The contour map of radii of the arcs of a Kerr naked singularity. (b) The contour map of central angles of the arcs. In the blank spaces (white areas) in (a) and (b), the arc does not exist.

Fig. 6.

We show the contour maps of the radius of the arc R_a and of its central angle ϑ_a in Fig. 7. As we see in Figs. 7(a) and (b), there is a blank space (a white area) in the right-bottom corner, in which the arc does not appear. It is because there exists no unstable spherical orbit with a positive radius in this area. From Fig. 7(a), we find that the radius increases as the inclination angle gets larger if the spin parameter is larger than $a \sim 1.1M$. This behavior is similar to the case of the radius of the black hole shadow (Fig. 4 (a)), except for the blank space.

The radius is finite in the neighborhood of the blank space, and vanishes discontinuously on the boundary.

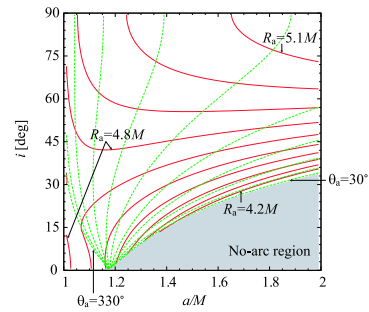


FIG. 8: The contour map of the radius of the arc R_a (the red solid curves) and its central angle ϑ_a (the green dashed curves). The contours are those for $R_a/M = 4.2, \dots, 5.1$, with the contour interval being 0.1 and $\vartheta_a = 30^\circ, \dots, 330^\circ$, with the contour interval being 30° . If one can observe ϑ_a and R_a , the spin parameter a of the Kerr naked singularity and the inclination angle i could be evaluated, although there exists a degenerate region near the blank space shaded in gray.

From Fig. 7(b), the central angle approaches 360° when both a spin parameter and an inclination angle are sufficiently small. That is to say, the arc closes and becomes a distorted “circle” in such parameter region. The central angle shows a steep decline to 0° in the neighborhood of the blank space. On the boundary, the arc vanishes with a finite radius.

In Fig. 8, we show the contour maps of the radius and of the central angle in terms of the spin parameter and inclination angle. Since these contours also give one-to-one correspondence between $(R_a$ and $\vartheta_a)$ and $(a$ and $i)$, we may be able to evaluate a spin parameter and an inclination angle by observing those two observables R_a and ϑ_a , just as the same as the case of a black hole.

When the inclination is larger than 45° (the upper half part of Fig. 8), one may easily determine the parameters a and i from the observation of R_a and ϑ_a . However, near the blank space, the contours of the spin parameter and the inclination angle become degenerate. One may find that it is hard to evaluate those parameters by real astronomical observations.

However, in the case of a naked singularity, we have an-

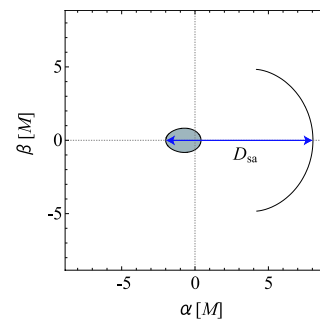


FIG. 9: The separation distance between the left endpoint of the dark spot and the center of the shadow, which we denote D_{sa} . We then define the aspect ratio of the shadow of a Kerr naked singularity; $\mathcal{A}_{sa} := D_{sa}/R_a$, where R_a is the arc radius.

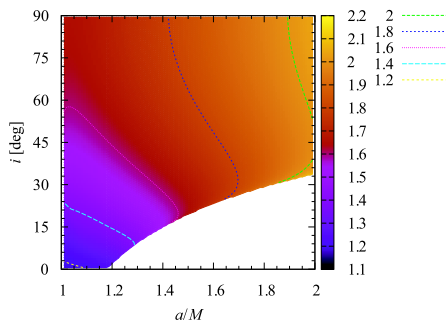


FIG. 10: The contour map of the aspect ratio of the shadow of a Kerr naked singularity, \mathcal{A}_{sa} .

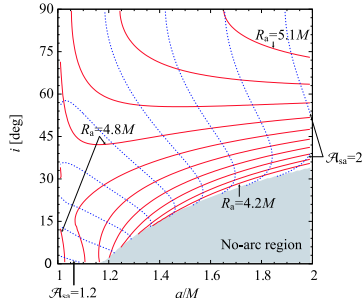


FIG. 11: The contour maps of the aspect ratio \mathcal{A}_{sa} (the blue dashed curves) and of the radius of the arc R_a (the red solid curves). The contours are those for $R_a/M = 4.2, \dots, 5.1$, with the contour interval being 0.1 and $\mathcal{A}_{\text{sa}} = 1.2, \dots, 2.0$, with the contour interval being 0.1. The one-to-one correspondence between (R_a and \mathcal{A}_{sa}) and (a and i) is very clear. We can use this contour map to determine the spin parameter and the inclination angle.

other part of the shadow, i.e., the dark spot (or the dark line). We can introduce another observable, the aspect ratio $\mathcal{A}_{\text{sa}} := D_{\text{sa}}/R_a$ by defining the separation distance between the left endpoint of the dark spot (or the left endpoint of the line) and the center of the arc, which we denote D_{sa} (see Fig. 9). We call \mathcal{A}_{sa} an aspect ratio since it is the ratio of the horizontal size of the shadow to the vertical one as a whole. We show the contour map of this observable in Fig. 10. This behavior is similar to the case of the deformation parameter of the black hole shadow (Fig. 4 (b)), except for the blank space. From Fig. 10, we find this aspect ratio \mathcal{A}_{sa} highly depends on a , which is very different from R_a . Hence a pair of R_a and \mathcal{A}_{sa} may be better to use for the determination of a and i . In fact, combining the two contour maps of R_a and \mathcal{A}_{sa} , we find a clear one-to-one correspondence as shown in Fig. 11. Hence if we observe both R_a and \mathcal{A}_{sa} , we can easily determine a and i .

Note that we may find one-to-two correspondence for

some parameters, e.g., $R_a/M = 4.8$ and $\mathcal{A}_{\text{sa}} = 1.6$. Even in that case, such information is still very useful because we have only two choices, e.g., $a/M = 1.21$ or 1.02 for the above data.

IV. CONCLUSION

A black hole casts a shadow as an optical appearance because of its strong gravitational field. The apparent shape of the shadow is distorted mainly by its spin parameter and the inclination angle. In this paper, we investigated whether it is possible to determine the spin parameter and the inclination angle by observing the apparent shape of the shadow of a compact object, which is assumed to be described by Kerr space-time. Introducing two observables, the radius R_s and the distortion parameter δ_s , characterizing the apparent shape, we found that the spin parameter and the inclination angle of a Kerr black hole can be determined by measuring those observables. It will rule out the possibility that a black hole candidate is a naked singularity, if we observe them. We have also extended this technique to the case of a Kerr naked singularity. The result may provide us with a practical method for future advanced interferometers.

Of course, we need further analysis to apply the present approach to realistic observations. First we have to evaluate the luminous flux in each direction. Then we can predict how dark in the directions around the shadow. It is especially important in the case of a naked singularity, because we have a one-dimensional dark arc as the shadow.

We usually expect that the light source is at a finite distance and the size is also finite such as an accretion disk. In that case, we may find shapes of shadows different from the present one. We should study several realistic light source models (a compact object with an accretion disk, or a gravitationally collapsing object, etc) in order to apply the present method. However, note that the present shape gives the region in which direction we can never observe any light from any light sources. Hence, even if we have more realistic light source, once we can find a part of the present shape, we may give some limits on the spin parameter and inclination angle.

Acknowledgements

This work was supported in part by the Grant-in-Aid for Scientific Research Fund of the JSPS Nos. 19540308 and 19-07795, and by the Japan-U.K. Research Cooperative Program.

[1] F. Eisenhauer *et al.*, *Astrophys. J.* **628**, 246 (2005) [arXiv:astro-ph/0502129].
 [2] Y. Tanaka *et al.*, *Nature* **375**, 659 (1995).

[3] C. S. Reynolds and M. A. Nowak, *Phys. Rept.* **377**, 389 (2003) [arXiv:astro-ph/0212065].
 [4] W. Cash, A. Shipley, S. Osterman and M. Joy, *Nature*

- 407**, 160 (2000).
- [5] H. Hirabayashi *et al.*, arXiv:astro-ph/0501020.
- [6] S. Doeleman *et al.*, *Nature* **455**, 78 (2008) [arXiv:0809.2442 [astro-ph]].
- [7] S. S. Doeleman, V. L. Fish, A. E. Broderick, A. Loeb and A. E. E. Rogers, *Astrophys. J.* **695**, 59 (2009) [arXiv:0809.3424 [astro-ph]].
- [8] J. M. Cunningham and C. T. Bardeen, *Astrophys. J.* **183**, 237 (1973).
- [9] K. S. Virbhadra and G. F. R. Ellis, *Phys. Rev. D* **62** (2000) 084003 [arXiv:astro-ph/9904193].
- [10] V. Bozza, *Phys. Rev. D* **66**, 103001 (2002) [arXiv:gr-qc/0208075].
- [11] V. Bozza, *Phys. Rev. D* **78**, 063014 (2008) [arXiv:0806.4102 [gr-qc]].
- [12] K. S. Virbhadra, *Phys. Rev. D* **79**, 083004 (2009) [arXiv:0810.2109 [gr-qc]].
- [13] A. F. Zakharov, *Class. Quant. Grav.* **11**, 1027 (1994).
- [14] A. F. Zakharov, F. De Paolis, G. Ingrosso and A. A. Nucita, *New Astron.* **10**, 479 (2005) [arXiv:astro-ph/0505286].
- [15] J. Schee and Z. Stuchlik, arXiv:0810.4445 [astro-ph].
- [16] C. Bambi and K. Freese, *Phys. Rev. D* **79**, 043002 (2009) [arXiv:0812.1328 [astro-ph]].
- [17] R. Penrose, *Ann. N. Y. Acad. Sci.* **224**, 125 (1973).
- [18] K. S. Virbhadra and G. F. R. Ellis, *Phys. Rev. D* **65**, 103004 (2002).
- [19] K. Nakao, N. Kobayashi and H. Ishihara, *Phys. Rev. D* **67**, 084002 (2003) [arXiv:gr-qc/0211061].
- [20] K. S. Virbhadra and C. R. Keeton, *Phys. Rev. D* **77**, 124014 (2008) [arXiv:0710.2333 [gr-qc]].
- [21] G. N. Gyulchev and S. S. Yazadjiev, *Phys. Rev. D* **78**, 083004 (2008) [arXiv:0806.3289 [gr-qc]].
- [22] H. Falcke, F. Melia and E. Agol, [*Astrophys. J.* **528**, L13 (2000)] arXiv:astro-ph/9912263.
- [23] R. Takahashi, *J. Korean Phys. Soc.* **45**, S1808 (2004) [*Astrophys. J.* **611**, 996 (2004)] [arXiv:astro-ph/0405099].
- [24] K. Beckwith and C. Done, *Mon. Not. Roy. Astron. Soc.* **359**, 1217 (2005) [arXiv:astro-ph/0411339].
- [25] A. E. Broderick and A. Loeb, *Astrophys. J.* **636**, L109 (2006) [arXiv:astro-ph/0508386].
- [26] A. E. Broderick and R. Narayan, *Astrophys. J.* **638**, L21 (2006) [arXiv:astro-ph/0512211].
- [27] R. Takahashi and K. Y. Watarai, *Mon. Not. Roy. Astron. Soc.* **374**, 1515 (2007) [arXiv:0704.2643 [astro-ph]].
- [28] S. M. Wu and T. G. Wang, *Mon. Not. Roy. Astron. Soc.* **378**, 841 (2007) [arXiv:0705.1796 [astro-ph]].
- [29] L. Huang, M. Cai, Z. Q. Shen and F. Yuan, *Mon. Not. Roy. Astron. Soc.* **379**, 833 (2007) [arXiv:astro-ph/0703254].
- [30] P. J. Young, *Phys. Rev. D* **14**, 3281 (1976).
- [31] A. de Vries, *Class. Quant. Grav.* **17**, 123 (2000).
- [32] K. Hioki and U. Miyamoto, *Phys. Rev. D* **78**, 044007 (2008) [arXiv:0805.3146 [gr-qc]].
- [33] C. W. Misner, K. S. Thorne, and J. A. Wheeler, *Gravitation*, (Freeman, 1973).
- [34] R. P. Kerr, *Phys. Rev. Lett.* **11**, 237 (1963).
- [35] K. Yano, *Ann. Math.* **55**, 328 (1952).
- [36] B. Carter, *Phys. Rev.* **174**, 1559 (1968).
- [37] S. Chandrasekhar, *The mathematical theory of black holes*, (Oxford Univ. Press, 1992) p. 646.
- [38] J. M. Bardeen, W. H. Press and S. A. Teukolsky, *Astrophys. J.* **178**, 347 (1972).
- [39] When we find the solution (19), we assume $r^2 + a^2 - a\xi \neq 0$. If $r^2 + a^2 - a\xi = 0$, i.e. $\xi = (r^2 + a^2)/a$, then we find $\mathcal{J} = 0$ for $\mathcal{R} = 0$. On the other hand, the condition for $\Theta \geq 0$ gives $\sin^2 \theta = \xi/a = (r^2 + a^2)/a^2 \geq 1$. The possible solution is $r = 0$ and $\theta = \pi/2$, which corresponds to the ring singularity. Hence we conclude that $r^2 + a^2 - a\xi \neq 0$.